Available online at www.sciencedirect.com
ScienceDirect
Trans. Nonferrous Met. Soc. China 22(2012) 825−830
Transactions of Nonferrous Metals Society of China
www.tnmsc.cn

Fretting wear and friction oxidation behavior of 0Cr20Ni32AlTi alloy at high temperature

ZHANG Xiao-yu[1], REN Ping-di[1], ZHONG Fa-chun[2], ZHU Min-hao[1], ZHOU Zhong-rong[1]

1. State Key Laboratory of Traction Power, Southwest Jiaotong University, Chengdu 610031, China;
2. Institute of Chemical Materials, Chinese Academy of Engineering and Physics, Mianyang 621900, China

Received 28 April 2011; accepted 28 July 2011

Abstract: The fretting wear behavior of 0Cr20Ni32AlTi alloy was investigated with crossed cylinder contact under 80 N at 300 and 400 °C. Wear scar and debris were analyzed systematically by scanning electron microscopy and X-ray photoelectron spectroscopy. The results show that the friction logs are mixed fretting regime and gross slip regime with the magnitudes of displacement of 10 and 20 μm, respectively. Severe wear and friction oxidation occur on the material surface. A large number of granular debris produced in the fretting process can be easily congregated and adhered at the contact zone after repeated crushes. The resultant of friction oxidation is mainly composed of Fe_3O_4, Fe_2O_3, Cr_2O_3 and NiO. Temperature and friction are the major factors affecting the oxidation reaction rate. The fretting friction effect can enhance the oxidation reaction activity of surface atoms of 0Cr20Ni32AlTi alloy and reduce the oxidation activation energy. As result, the oxidation reaction rate is accelerated.

Key words: high temperature; nickel chrome-iron alloy; fretting wear; friction oxidation; activation energy

1 Introduction

Fretting is a wear phenomenon occurring when two contact surfaces are subjected to small amplitude oscillatory movement, which can accelerate crack nucleation of working components and lead to premature catastrophic failures [1,2]. Fretting has become one of the major causes leading to tight fit assembly and clearance fit assembly failures in nuclear power systems. A large number of fretting damages [3] exist and appear at various parts of nuclear power systems, such as reactor fuel assembly, control rod assembly, reactor component, steam generator, pressure vessel, main pump and coolant pump. Steam generator is the key equipment in nuclear power systems and fretting damage is one of the main reasons [4] which cause component failure. With high thermal strength, good corrosion resistance, antioxidation and other characteristics, 0Cr20Ni32AlTi alloy is widely used in the nuclear power and aerospace fields. Nowadays, it becomes one of three main materials applied for nuclear steam generator tubes. Its performance plays an important role in the safe operation of nuclear power stations. Effects of working conditions, organizational structure [5,6], composition [7] and other factors [8−16] on friction and wear properties of 0Cr20Ni32AlTi alloy have been researched using micro-analysis equipment, while relatively less work has been carried out on the fretting damage mechanism, friction oxidation and debris component change.

In this work, the fretting damage morphology, debris morphology and chemical composition of 0Cr20Ni32AlTi alloy were studied at high temperature. The kinetics law of oxidation conversion reaction for wear debris was analyzed by calculating the activation energy.

2 Experimental

A hydraulic fretting wear test rig was used to test the fretting wear behaviors of 0Cr20Ni32AlTi alloy with crossed cylinder contact. As seen in Fig. 1, the cylinder specimen was mounted on a ball, which was fixed to the upper holder and moved with the piston of the hydraulic

Foundation item: Project (51075342) supported by the National Natural Science Foundation of China; Project (2007CB714704) supported by the National Basic Research Program of China
Corresponding author: REN Ping-di; Tel: +86-28-87600226; E-mail: rpd@swjtu.edu.cn
DOI: 10.1016/S1003-6326(11)61251-X

system. The cylinder specimen was fixed on the lower holder, which was mounted on the specimen chamber. Cyclic movement between the contact pairs was measured and controlled by the extensometer. Normal load (F_n) was applied to the clamp of the ball by a weight set through a wire. The friction force was measured by the sensor of load cell. During the fretting test, the variations of tangential force vs. displacement as a function of fretting cycles can be recorded.

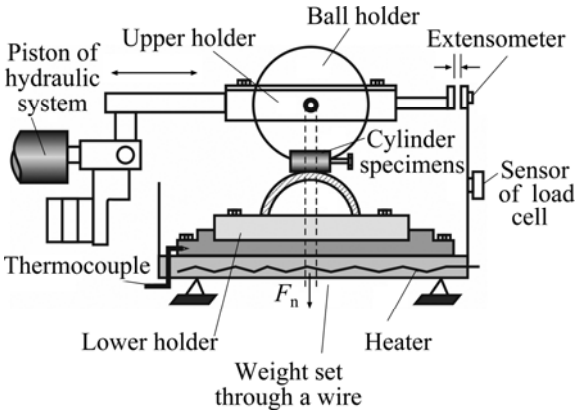

Fig. 1 Schematic diagram of fretting wear test

The cylinder specimens of 0Cr20Ni32AlTi alloy were machined to a size of *d*22 mm×10 mm, and the thickness (δ) of the pipe wall was 1.2 mm. The surfaces were carefully polished to a final roughness (R_a) of about 0.02 μm. 0Cr18Ni9 stainless steel cylinder with size of *d*10 mm×10 mm, and surface roughness of 0.02 μm was used as the counterparts. Prior to the fretting tests, the specimens were ultrasonically cleaned with acetone and thoroughly dried. The chemical composition of the specimen is listed in Table 1.

Table 1 Chemical composition of 0Cr20Ni32AlTi alloy (mass fraction, %)

C	Si	Mn	Ni	Cr	Ti
0.02	0.35	1.00	32	21.0	0.4

Al	Cu	S	P	Fe
0.4	0.3	0.01	0.02	Bal.

The experimental parameters for the fretting wear tests were as follows: normal load (F_n) of 80 N, displacement amplitude (*D*) of 10 and 20 μm respectively at constant frequency of 2 Hz, number of cycles (*N*) of 3×10^4. The fretting wear tests were conducted at high temperature under an ambient atmospheric condition (50%−60% relative humidity). The required temperature was realized using heating elements placed into the lower holder. The temperature was measured by means of a thin thermocouple placed at the top of the flank surface of the lower specimen. The friction surface of the upper specimen was heated by the lower specimen due to thermal conductivity. In order to maintain the setting temperature constant, a programmable controller was used to control the variation of temperature and homogenize the temperature. During the test, the actual temperature exhibited certain extent fluctuation around the setting temperature. At the setting temperature of 300 °C, the temperature was steady at a range of ±2 °C. The fluctuation of the temperature range was about ±5 °C at the setting temperature of 400 °C. So, before each test, the contact area was preheated for 40 min to decrease the differences between the actual and the setting temperatures.

After the fretting wear tests, the morphologies of the worn scars were examined by scanning electron microscopy (SEM, Quanta2000), and the chemical compositions were analyzed by X-ray photo electron spectroscopy (XPS, PHI−5702).

3 Results and discussion

3.1 Morphology of wear scars

Under the imposed normal of 80 N and displacement amplitudes of 10 and 20 μm, the fretting processes run in mixed fretting regime (MFR) and slip regime (SR) [17,18], and the increasing temperature does not obviously influence the fretting regime features. The micrographs of the wear scars of the 0Cr20Ni32AlTi alloy in MFR and SR at different temperatures are shown in Fig. 2. In MFR (*D*=10 μm), the granular debris layer are congregated at the contact zone, as shown in Figs. 2(a) and (c). The oxide content of alloying elements of debris layer increases at high temperature (400 °C), and the friction-reducing effect of debris layer is improved. In SR (*D*=10 μm), the scar morphology becomes more and more serious as the displacement amplitude increases. During the migration process, the debris forms the third body layer [19,20] with strong bearing capacity by reciprocating roller compaction, which covers the contact surface.

3.2 Composition of wear debris

Figure 3 depicts the composition profile of the main elements in 0Cr20Ni32AlTi alloy at the worn zone under different temperatures. The oxygen content of the debris layer decreases slowly with the increase of sputter depth and gradually becomes stable. The iron content of the debris layer increases as this change of sputter depth and tends to be stable. The nickel and chrome contents of the debris layer little change with the increase of sputter

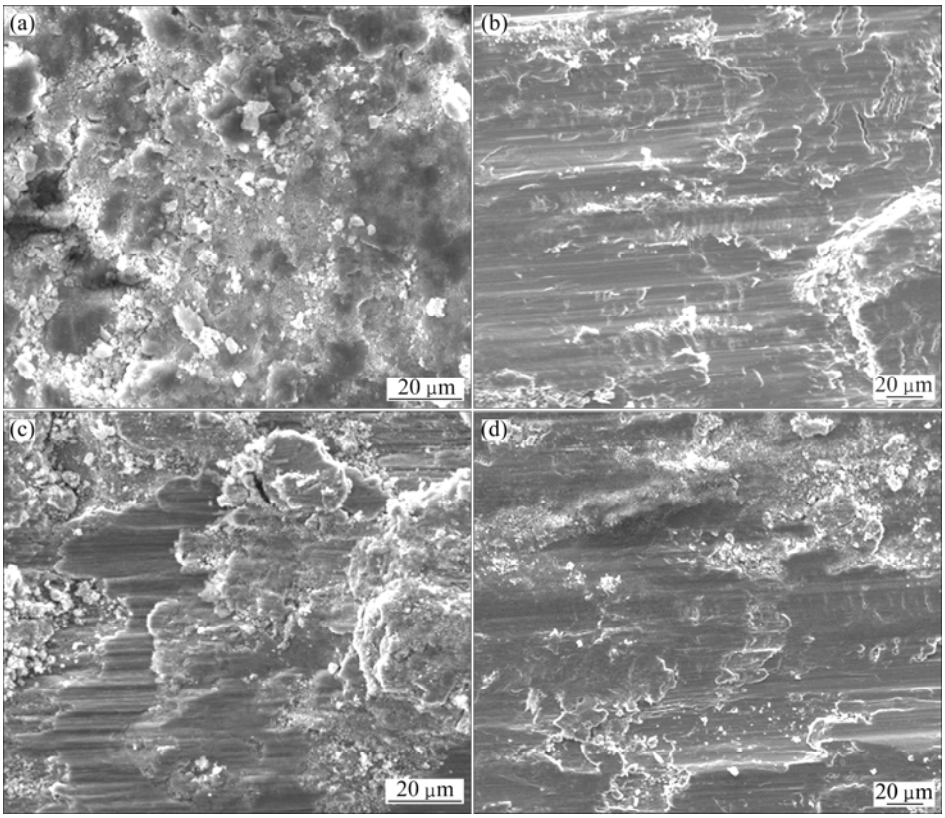

Fig. 2 SEM morphologies of wear scars of 0Cr20Ni32AlTi alloy under different conditions: (a) D=10 μm, t=300 °C ; (b) D=20 μm, t=300 °C; (c) D=10 μm, t=400 °C ; (d) D=20 μm, t=400 °C

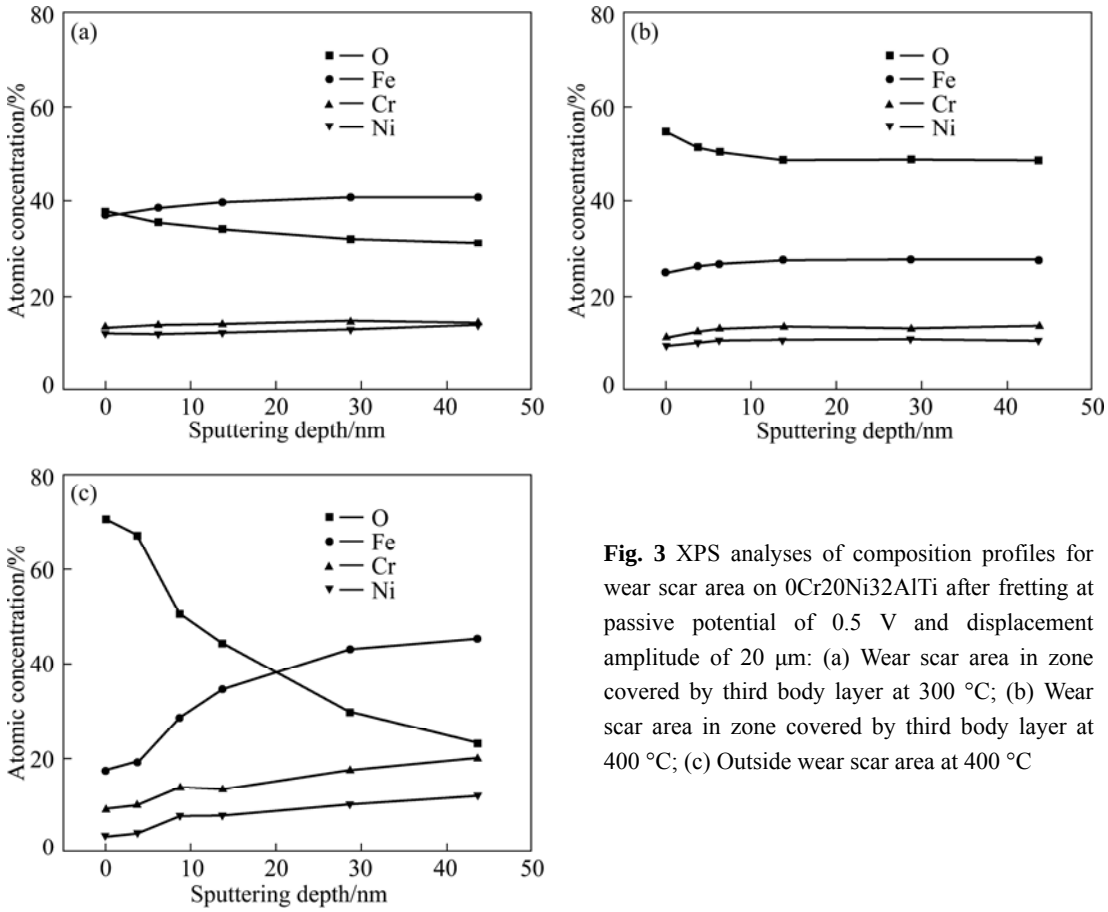

Fig. 3 XPS analyses of composition profiles for wear scar area on 0Cr20Ni32AlTi after fretting at passive potential of 0.5 V and displacement amplitude of 20 μm: (a) Wear scar area in zone covered by third body layer at 300 °C; (b) Wear scar area in zone covered by third body layer at 400 °C; (c) Outside wear scar area at 400 °C

depth (as shown in Fig. 3(a)). The oxygen content in the debris layer decreases with increasing sputter depth and becomes stable, while iron, nickel and chrome contents increase with this change of sputter depth and do not vary obviously (Fig. 3(b)). The oxygen content of the debris layer decreases quickly with the increase of sputter depth and gradually becomes stable. At the same time, iron, nickel and chrome contents increase with this change of sputter depth (as shown in Fig. 3(c)).

The oxygen content in Fig. 3(b) is significantly higher than that in Fig. 3(a). The oxidation reaction rate accelerates with increasing temperature, and the oxide content increases. Fe, Ni, Cr and other alloying elements contents are relatively lower because of the involvement in oxygen. However, the oxygen content in Fig. 3(c) is significantly lower than that in Fig. 3(b) with sputtering depth of 9.75 nm. So temperature and friction are the major factors affecting the friction oxidation reaction rate. The oxidation reaction rate is accelerated by the combined effect of two factors that are the decrease of oxidation activation energy and the increase of oxidation reaction activity in the friction processes.

In order to quantitatively analyze the oxide content of main alloying elements in the debris, the XPS spectra of Fe, Ni, Cr and other elements were dealt with sub-peak fitting. The XPS spectra of Fe 2p, Ni 2p and Cr 2p on the worn surfaces are shown in Fig. 4.

The XPS spectra of Fe 2p on the worn surfaces are shown in Fig. 4(a). The Fe $2p_{3/2}$ spectrum is decomposed according to the procedure described in Ref. [21]. On the worn surfaces of 0Cr20Ni32AlTi, iron is presented in the forms of Fe^0, Fe^{2+} and Fe^{3+} (E_b =706.8, 708.5 and 711.1 eV, respectively) as in the composition of Fe, Fe_3O_4 and Fe_2O_3.

The XPS spectra of Ni 2p on the worn surfaces are shown in Fig. 4(b). The shape of the band and the binding energies of Ni $2p_{3/2}$ electrons suggest that nickel presents on the worn surfaces of 0Cr20Ni32AlTi in the forms of Ni^0 and Ni^{2+} (E_b=852.3, 854.2 and 858.1 eV respectively). It forms Ni, NiO and $Ni(OH)_2$ [22].

The XPS spectra of Cr 2p on the worn surfaces are shown in Fig. 4(c). For peak fitting analysis of Cr $2p_{3/2}$ spectrum, the Cr $2p_{3/2}$ XPS that appears at peak binding energy of 573.6 and 576.3 eV corresponds to the formation of Cr and Cr_2O_3, respectively [23].

The oxide content of alloying elements could be quantitatively calculated and obtained by integral areas of the characteristic peaks of oxides, as listed in Table 2.

3.3 Activation energy of friction oxidation reaction

The oxides of the three main alloying elements (Cr、Ni and Fe) are formed according to the following oxidation reaction: $4Cr+3O_2=2Cr_2O_3$, $2Ni+O_2=2NiO$,

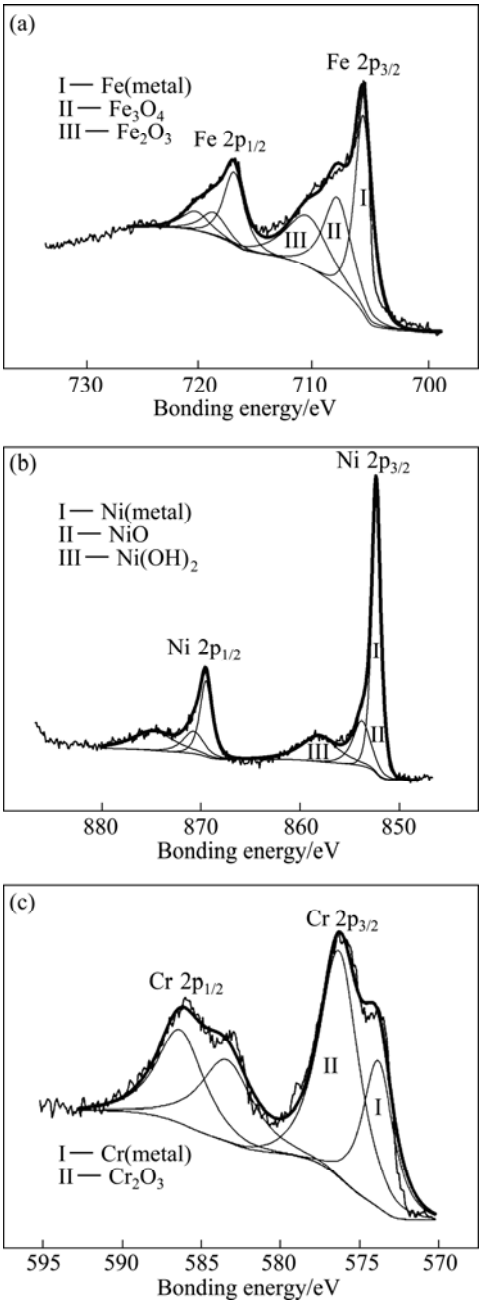

Fig. 4 XPS spectra of Fe 2p, Ni 2p and Cr 2p for wear scar area on 0Cr20Ni32AlTi at 300 °C for sputtering time of 175 s with displacement amplitude of 20 μm: (a) Fe 2p; (b) Ni 2p; (c) Cr 2p

Table 2 Oxide contents of wear debris of 0Cr20Ni32AlTi alloy

Test condition	$w(Fe_3O_4)$/%	$w(Fe_2O_3)$/%	w(NiO)/%	$w(Cr_2O_3)$/%
Non-worn zone, t=300 °C	15.1	0	2.69	7.43
Non-worn zone, t=400 °C	29	0	5.77	13.1
Worn zone, t=300 °C	20.1	19.48	12.50	19.54
Worn zone, t=400 °C	19.53	35.44	14.73	26.75

Table 3 Oxidation reaction rate and activation energy

Test condition	Reaction rate/(10^{-4}min^{-1})				Activation energy/(kJ·mol^{-1})			
	Cr_2O_3	NiO	Fe_3O_4	Fe_2O_3	$\alpha(Cr_2O_3)$	α(NiO)	$\alpha(Fe_3O_4)$	$\alpha(Fe_2O_3)$
Non-worn zone, t=300 °C	2.129	0.78	4.56	−	14.32	20.71	17.18	−
Non-worn zone, t=400 °C	3.238	1.488	7.792	−	14.32	20.71	17.18	−
Worn zone, t=300 °C	2.872	1.272	5.16	4.496	10.73	17.04	4.13	13.32
Worn zone, t=400 °C	5.412	2.164	10.98	6.812	10.73	17.04	4.13	13.32

$3Fe+2O_2$═Fe_3O_4 and $4Fe_3O_4+O_2$═$6Fe_2O_3$. The relevant oxidation reaction rate and rate constant could be calculated in terms of the oxide content of alloying elements and the test time of fretting wear (see Table 2). The oxidation activation energy with the Arrhenius formula could be obtained according to the oxidation reaction rate and rate constant in the same reaction at different temperatures. The calculation results of the oxidation reaction rate and activation energy are listed in Table 3.

The oxidation reaction rate of the three main alloying elements (Cr, Ni and Fe) increases significantly with the increase of test temperature. This result is consistent with Arrhenius equation: $k=A\exp(-E_a/RT)$, where K is the reaction rate constant; E_a is the activation energy; R is the Boltzmann constant and T is the temperature in Kelvin, which describes the relationship between the reaction rate constant and temperature. According to the calculation analysis of the reaction rate and activation energy, the reaction rate is faster in the worn zone than in the non-worn zone in the same oxidation reaction at a given temperature. Therefore, friction effect enhances the activity of the metal surface, and accelerates the oxidation reaction rate. The analysis of calculation results of activation energy for several major oxidation reactions show that the friction effect can improve the oxidation reaction activity and more importantly reduce the oxidation activation energy. With the increase of the oxidation reaction rate and rate constant, oxidation reaction is accelerated according to the Arrhenius formula. Fe is more easily oxidized among the alloying elements, and it has larger oxidation reaction rate and lower activation energy. Ni is harder to be oxidized than Fe. The oxidized characteristic of Cr is between Ni and Fe. The law of metal activity order is not entirely consistent with the order of Cr, Fe and Ni. The oxides of Fe are mainly composed of Fe_3O_4 and Fe_2O_3 [24]. According to the analysis of the calculation data, the oxidation reaction $3Fe+2O_2$═Fe_3O_4 is easier to occur than $4Fe_3O_4+O_2$═ $6Fe_2O_3$.

With the increase of temperature, the value of rate constant k increases, and the reaction rate is accelerated in the above oxidation reaction. So, temperature is an important factor affecting the chemical reaction rate. When the temperature is 300 or 400 °C, the oxidation reaction activity of alloying elements is affected by the initial reaction film of material surface. Due to the effect of frictional shear stress, the initial film of material surface is eliminated, and the contacting surfaces exchange matter and energy with the environment. Particularly, the oxidation reaction activity of surface atoms of 0Cr20Ni32AlTi alloy is enhanced. At the same time, the friction effect reduces the oxidation activation energy [25]. The oxidation reaction rate is significantly accelerated by the combined effect of two factors that are the decrease of oxidation activation energy and the increase of oxidation reaction activity in the friction processes. Therefore, temperature and friction effect are the two major factors affecting the friction oxidation reaction rate.

4 Conclusions

1) Severe damage and friction oxidation occur in the mixed fretting regime and gross slip regime. A large number of the debris layers produced during the fretting wear processes could be easily congregated and adhered at the contact zone. The resultant of friction oxidation reaction could be mainly composed of metal oxides.

2) Temperature and friction effect are the major factors affecting the friction oxidation reaction rate. The oxidation reaction rate is accelerated by the combined effect of two factors, the decrease of oxidation activation energy and the increase of oxidation reaction activity in the friction processes.

References

[1] TAYLOR D E, HARDISTY F B, WATERHOUSER B, NEHRU A Y. The fretting wear of an austenitic stainless steel in air and in carbon dioxide at elevated temperatures [J]. Wear, 1979, 56(1): 9−18.

[2] KAYABA T, IWABUCHI A. The fretting wear of 0.45%C steel and austenitic stainless steel from 20 to 650 °C in air [J]. Wear, 1981, 74(2): 229−245.

[3] TANG Hui. Fretting damage one of world wide difficulties in the field of nuclear power equipment and structures for a long term [J]. Nuclear Power Engineering, 2000, 21(3): 222−231.

[4] LOW M B J. Fretting problems and some solutions in power plant machinery [J]. Wear, 1985, 106(1−3): 315−336.

[5] HONG K J, KIM I S, PARK C Y, KIM E S. Microstructural effects

on the fretting wear of Inconel 690 steam generator tube [J]. Wear, 2005, 259(1−6): 349−355.
[6] HU J, LI D Y, LLEWELLYN R. Synergistic effects of microstructure and abrasion condition on abrasive wear of composites–A modeling study [J]. Wear, 2007, 263(1−6): 218−227.
[7] MONTERMOR M F, FERREIRA M G S, HAKIKI N E, DA C H B M. Chemical compostion and electronic structure of the oxide films formed on 316L stainless steel and nickel based alloys in high temperature aqueous environments [J]. Corrosion Science, 2000, 42(9): 1635−1650.
[8] HONG S M, KIM I S. Impact fretting wear of alloy 690 tubes at 25 and 290 °C [J]. Wear, 2005, 259(1−6): 356−360.
[9] STOTT F H, LIN D S, WOOD G C, STEVENSON C W, The tribological behaviour of nickel and alloys at temperatures from 20 to 800 °C [J]. Wear, 1976, 36(2): 147−174.
[10] YUCEL B. High temperature sliding wear behaviour of Inconel 617 and Stellite 6 alloys [J]. Wear, 2010, 269(9−10): 664−671.
[11] NICKCHI T, ALFANTAZI A. Electrochemical corrosion behaviour of Incoloy 800 in sulphate solutions containing hydrogen peroxide [J]. Corrosion Science, 2010, 52(12): 4035−4045.
[12] MENG Fan-jiang, WANG Jian-qiu, HAN En-hou, KE Wei. The role of TiN inclusions in stress corrosion crack initiation for alloy 690TT in high-temperature and high-pressure water [J]. Corrosion Science, 2010, 52(3): 927−932.
[13] KAAE J L. High-temperature low-cycle fatigue of alloy 800H [J]. International Journal of Fatigue, 2009, 31(2): 332−340.
[14] KWON J D, JEUNG H K, CHUNG I S, YOON D H, PARK D K. A study on fretting fatigue characteristics of Inconel 690 at high temperature [J]. Tribology International, 2011, 44(1): 1483−1487.
[15] ZHANG Y D, ZHANG C, LAN H, HOU PY, YANG Z G. Improvement of the oxidation resistance of Tribaloy T−800 alloy by the additions of yttrium and aluminium [J]. Corrosion Science, 2011, 53(3): 1035−1043.
[16] INMAN I A, DATTA P S, Studies of high temperature sliding wear of metallic dissimilar interfaces III: Incoloy MA956 versus Incoloy 800 HT [J]. Tribology International, 2010, 43(11): 2051−2057.
[17] ZHOU Z R, VINCENT L. Mixed fretting regime [J]. Wear, 1995, 181–183(11−12): 531−536.
[18] ZHOU Z R, FAYEULLE S, VINCENT L. Cracking behaviour of various aluminum alloys during fretting wear [J]. Wear, 1992, 155 (2): 317−330.
[19] MϕLgaard J. A discussion of oxidation, oxide thickness and oxide transfer in wear [J]. Wear, 1976, 40(3): 277−291.
[20] ZHANG Xiao-yu, REN Ping-di, ZHANG Ya-fei, ZHU Min-hao, ZHOU Zhong-rong. Fretting wear behavior of Incoloy 800 alloy at high temperature [J]. The Chinese Journal of Nonferrous Metals, 2010, 20(8): 1545−1551. (in Chinese)
[21] TORU Y, PETER H. Analysis of XPS spectra of Fe^{2+} and Fe^{3+} ions in oxide materials [J]. Applied Surface Science, 2008, 254(8): 2441−2449.
[22] GROSVENOR A P, BIESINGER M C, SMART R S C, MCINTYRE N S. New interpretations of XPS spectra of nickel metal and oxides [J]. Surface Science, 2006, 600(9): 1771−1779.
[23] PAYNE B P, BIESINGER M C, MCINTYRE N S. X-ray photoelectron spectroscopy studies of reactions on chromium metal and chromium oxide surfaces [J]. Journal of Electron Spectroscopy and Related Phenomena, 2011, 184(1−2): 29−37.
[24] WANG F, CUI X H, YANG Z R, WEI M X, WANG S Q. Oxidation and tribo-oxidation of an alloy steel H13 at elevated temperature [J]. Journal of Engineering Tribology, 2009, 233(6): 881−885.
[25] MϕLgaard J, SRIVASTAVA V K. The activation energy of oxidation in wear [J]. Wear, 1977, 41(2): 263−270.

0Cr20Ni32AlTi 合金的高温微动磨损及摩擦氧化特性

张晓宇[1]，任平弟[1]，钟发春[2]，朱旻昊[1]，周仲荣[1]

1. 西南交通大学 牵引动力国家重点实验室，成都 610031；
2. 中国工程物理研究院 化工材料研究所，绵阳 621900

摘　要：在 300 和 400 ℃、载荷 80 N 的条件下，将 0Cr20Ni32AlTi 合金以水平垂直交叉接触方式进行微动磨损试验，并采用 SEM 和 XPS 对磨痕及磨屑进行分析。结果表明：当位移幅值为 10 和 20 μm 时，微动分别对应于混合区和滑移区，且材料表面均发生严重的磨损和摩擦氧化。微动过程产生大量颗粒状磨屑，经往复碾压后易粘附、聚集于接触区。摩擦氧化反应的生成物主要由 Fe_3O_4、Fe_2O_3、Cr_2O_3 和 NiO 等组成。温度和摩擦作用是影响磨屑氧化转化反应速率的主要因素。微动摩擦作用可以增加 0Cr20Ni32AlTi 合金表面原子的氧化反应活性并降低氧化反应的活化能，从而加快磨屑氧化转化反应的速率。

关键词：高温；镍铬铁合金；微动磨损；摩擦氧化；活化能

(Edited by FANG Jing-hua)